IEEE Access
Multidisciplinary | Rapid Review | Open Access Journal

Received November 8, 2021, accepted November 18, 2021, date of publication November 23, 2021,
date of current version December 7, 2021.

Digital Object Identifier 10.1109/ACCESS.2021.3130216

Application of a New CO_2 Prediction Method Within Family House Occupancy Monitoring

JAN VANUS, OJAN MAJIDZADEH GORJANI, PETR DVORACEK, PETR BILIK, AND JIRI KOZIOREK

Department of Cybernetics and Biomedical Engineering, Faculty of Electrical Engineering and Computer Science, VSB—Technical University of Ostrava, 70800 Ostrava, Czech Republic

Corresponding author: Ojan Majidzadeh Gorjani (ojan.majidzadeh.gorjani@vsb.cz)

This work was supported in part by the European Union's Horizon 2020 Research and Innovation Program under Grant NO856670, in part by the European Regional Development Fund in "A Research Platform focused on Industry 4.0 and Robotics in Ostrava Agglomeration" Project, through the Operational Program Research, Development and Education, under Grant CZ.02.1.01/0.0/0.0/17_049/0008425, and in part by the "Student Grant System" of VSB—TU Ostrava under Project SP2021/123.

ABSTRACT The article describes the application of Python for verification of a newly designed method of CO_2 prediction from measurements of indoor parameters of temperature and relative humidity within occupancy monitoring in real conditions of a family home. The article describes the implementation of non-electric quantities (indoor CO_2 concentration, indoor temperature, indoor relative humidity) measurement in five rooms of a family home (living room, kitchen, children's room, bathroom, bedroom) using Loxone technology sensors. The IBM IoT (Internet Of Things) was used for storing and subsequent processing of the measured values within the time interval of December 22, 2018, to December 31, 2018. The devised method used radial basis function (artificial neural networks (ANN)) mathematical method (implementation in Python environment) to perform accurate predictions. For further increase of the accuracy and reduction of prediction noise from the obtained course of the predicted signal, multiple variations of the LMS adaptive filter algorithm (Sign, Sign-Sign, Sign-Regressor) were used (implemented in the MATLAB SW tool). The accuracy of the newly proposed CO_2 concentration prediction method exceeds 95% in the selected experiments.

INDEX TERMS Artificial neural network (ANN), intelligent buildings (IB), Loxone, monitoring, occupancy, prediction, smart home (SH).

I. INTRODUCTION

The technologies used to manage and control smart buildings and smart homes (SH) are undergoing very rapid development due to their increasing popularity among investors. Building management is most often used for energy savings that can be achieved by optimum regulation. Therefore, the current research very often addresses the issue of energy saving with micro-grid networks [1]–[3], HEMS (Home Energy Management System) [4], KNX (Konnex) system elements [5]–[11], by regulating artificial lighting based on daylight intensity [12]–[14], the possibility of simplifying the required communications among the user interface level and the individual devices using unified communication protocols [15][11], IoT platform [16]–[18], a solution for interconnecting the devices used in SH running on different platforms by means of Android devices [19], wireless devices [20]–[22], a single distributed control system using IPv6 for creating a concept of Smart (or Interconnected) Cities [23].

Markiewicz [9] describes a language that can be used to plan daily routines of house occupants and that can be easily understood by an average user and can be easily interpreted for microcontroller processors. As mentioned in the previous paragraphs, SH systems are also used in homes with extended care for the elderly and physically and mentally handicapped. Arnold *et al.* [24] discuss the issue of making the control of SH systems for the elderly available by means

The associate editor coordinating the review of this manuscript and approving it for publication was Liang-Bi Chen.

of platforms that communicate using the common language and are able to analyze it. The use of CO_2 concentration measurements in SH is one area that is also mentioned in this work. Brennan *et al.* [25] propose a solution that enables detection of people presence based on CO_2 concentration. Khazaei *et al.* [26] and Skon *et al.* [27] deal with indirect measurement of CO_2 concentration by neural networks. Vanus *et al.* [28]–[30] also deal with the same issue. They came with the solution of the on-line prediction of CO_2 concentration by connecting to the IBM SPSS IoT platform. The use of CO_2 concentration measurement for room occupancy monitoring is suggested because the concentration of this gas is often monitored in buildings for health-related reasons, and not only commercial buildings are increasingly equipped with sensors for direct CO_2 concentration measurement in order to control HVAC (Heating, Ventilation and Air Condition). The assumed fact that the source of CO_2 in the room is only of a human (and, to a lesser extent, also of an animal) is another reason for using CO_2 as an indicator of presence. The value of CO_2 concentration in the atmosphere is constantly changing, the average value of CO_2 concentration is around 400 ppm [31]. During the breathing process, the oxy-gen contained in the air is inhaled and converted to CO_2. The air a human exhales contains, on average, 35,000–50,000 ppm amount of CO_2; this is approximately 100 times more than the concentration in the atmosphere. This fact allows us to detect the presence of people in the room based on the progression of the CO_2 concentration and also to determine their number based on the steepness of its gradient. The disadvantage of using CO_2 as an indicator of presence may be seen in the costliness of the sensors for the direct measurement of CO_2 and, also, the fact that these sensors are still not standard equipment of intelligent buildings and are often installed only where it is necessary to monitor CO_2 concentration directly, for example, due to health reasons. For this reason, Vanus *et al.* [29] have come up with a solution that uses an artificial neural network to indirectly measure CO_2 concentration based on temperature outdoor, temperature indoor, and air humidity in the room, which are the values that are mostly monitored in any intelligent building and for which the acquisition cost of the sensors is by an order of magnitude lower than that of sensors for direct CO_2 measurement.

The use of CO_2 concentration measurement for room occupancy monitoring is suggested because the concentration of this gas is often monitored in buildings for health-related reasons, and not only commercial buildings are increasingly equipped with sensors for direct CO_2 concentration measurement in order to control HVAC (Heating, Ventilation and Air Condition). The assumed fact that the source of CO_2 in the room is only of a human (and, to a lesser extent, also of an animal) is another reason for using CO_2 as an indicator of presence. The value of CO_2 concentration in the atmosphere is constantly changing, the average value of CO_2 concentration is around 400 ppm [31]. During the breathing process, the oxy-gen contained in the air is inhaled and converted to CO_2. The air a human exhales contains, on average, 35,000–50,000 ppm amount of CO_2; this is approximately 100 times more than the concentration in the atmosphere. This fact allows us to detect the presence of people in the room based on the progression of the CO_2 concentration and also to determine their number based on the steepness of its gradient. The disadvantage of using CO_2 as an indicator of presence may be seen in the costliness of the sensors for the direct measurement of CO_2 and, also, the fact that these sensors are still not standard equipment of intelligent buildings and are often installed only where it is necessary to monitor CO_2 concentration directly, for example, due to health reasons. For this reason, Vanus *et al.* [29] have come up with a solution that uses an artificial neural network to indirectly measure CO_2 concentration based on temperature outdoor, temperature indoor, and air humidity in the room, which are the values that are mostly monitored in any intelligent building and for which the acquisition cost of the sensors is by an order of magnitude lower than that of sensors for direct CO_2 measurement.

In this article, individual Loxone sensors will be used to measure the required non-electric indoor quantities (5 pieces of CO_2 concentration sensors, 5 pieces of temperature sensors, 5 pieces of relative humidity sensors) for occupancy estimation. The objective of this article is to verify the possibilities of using the Python development environment to create a new method for obtaining the CO_2 prediction using the measured indoor values of temperature and indoor relative humidity inside a real family home within occupancy recognition monitoring. The article has used ANN radial basic function (RBF) mathematical method as a predictive model and for increasing the accuracy by suppressing the prediction noise from a predicted signal using multiple variations of the LMS adaptive filter algorithm (Sign, Sign-Sign, Signed-Regressor). The experiments were conducted from December 22, 2018, to December 31, 2018, in five rooms of a family home: ''living room, children's room, bedroom, kitchen, and bathroom''. Another goal was to verify the functionality and accuracy of this newly devised CO_2 concentration prediction method for the specific areas of a family home (kitchen, bathroom), in which the source of moisture and CO_2 concentration is not only the humans but also the consequences of human activities that come to existence during cooking or showering.

II. RELATED WORK

Occupancy patterns are necessary to estimate energy demand and evaluate thermal comfort in households [32]. Chen performed a comprehensive review on occupancy estimation and detection and categorized the systems based on the use of different sensors, such as PIR, smart meter, environmental sensors (CO_2, relative humidity, temperature, pressure, illuminance), camera, WiFi, BLE, and others [33]. Azizi analyzed the data from the PIR sensors and the booking system in 8 lecture halls in a University building and estimated for the case study that the intervention to close down redundant lecture halls to improve space use efficiency

can result in a 19% reduction of energy use of lecture halls [34]. Becker's aim in their work was to advocate unsupervised classification algorithms for occupancy detection in private households which use the electricity consumption data measured by smart meters with best-performing algorithms showed an accuracy of 69–90% or an MCC of 0.20–0.78 [35]. Candanedo presents and evaluates a simple methodology based on Hidden Markov Models for the problem of unsupervised occupancy detection using different environmental parameters such as temperature, humidity, humidity ratio, CO_2, and light time series data with an accuracy of 90.24% [36]. A methodology, aimed at implementing an occupancy-based HVAC system operation schedule, is presented by Capozzoli. The savings related to the energy consumption of the HVAC system, as a result of the implementation of the strategy, in comparison to an occupancy-independent operation schedule amounted to 14% [37]. Dong proposes three different occupancy prediction methods (proposed short-term stochastic modeling methods, GSPS, EM, and uncertain basis) for demand-based HVAC control with achieved more than 70% accuracy in the experimental studies [38].

III. MATERIALS AND METHODS

In works [30], [39], IBM SPSS Modeler has been used to implement radial basis functions (feedforward neural networks) for CO_2 prediction. These papers investigated the accuracy and performance of the trained models according to the number of neurons in the hidden layer and the length of the training intervals. The result indicated that the training intervals with a length of one day are producing the most accurate outcomes. In this article, the proposed method (Figure 1) contains multiple parts. In the first part, the measurement and data collection were performed using Loxone technology. The second part contains predictive analytics implemented using TensorFlow and Keras within the Python programming language (Figure 2). For storage and visualization (using MQTT Gateway software similar to the solution used in work [40]), the predictions and measured values are sent to the IBM Watson IoT platform. In addition to the novel methodology, the paper investigates the accuracy of the measurements in a variety of locations within a smart home.

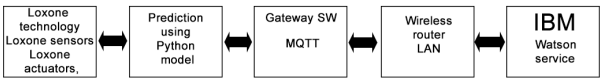

FIGURE 1. General block diagram of the proposed solution.

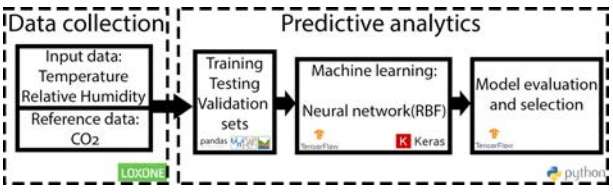

FIGURE 2. General diagram of the predictive model development.

A. MEASUREMENTS AND DATA COLLECTION USING LOXONE TECHNOLOGY

Loxone components were used for the actual measurements. The Loxone system is a centralized system, the main element of which is the PLC Loxone Miniserver [41]. Other rack peripherals, such as DMX, EnOcean or DALI extensions, connect to the Loxone Miniserver via the Loxone Link bus. Other rack peripherals, such as DMX, EnOcean or DALI extensions, connect to the Loxone Miniserver via the Loxone Link bus. A new feature in the Loxone system includes the Loxone Tree bus, which is used for the bus connection of sensors and actuators to the Miniserver, which has, so far, been implemented using separate cabling for each of these elements.

The Loxone Miniserver is the central component of the Loxone system. It is a powerful PLC that also includes basic connectivity. Loxone Config software is used to configure the program for the Loxone Miniserver. The Loxone Miniserver is available in two versions – the DIN version for mounting on the rack rail and the Go version, which is designed especially for the additional conversion of a conventional electrical installation to an intelligent one. The basic technical parameters of the Loxone Miniserver (in DIN rail version) are:

- 8× switching outputs relays for connection of blinds or lights.
- 8× digital inputs for connecting push buttons, door and window contacts, etc.
- 4× analogue inputs for connection of sensors, such as temperature, humidity, etc.
- 4× analogue outputs for connection of drives etc.
- LAN interface for controlling network devices, such as TV, etc.
- KNX / EIB interface.
- Up to 30 extension modules using Loxone Link.
- Power supply: 24 V DC.

The Loxone Miniserver can be connected to other peripherals that enhance the basic connectivity or functionality of the Miniserver using the Loxone Link bus. Loxone often extends the range of these elements. The following section describes those peripherals that have applications in the areas described in other sections of this work, especially lighting and HVAC. To ideally control the technical and operational functions of smart homes, it is necessary to have sufficient data available that can be used either for the direct control of some of the functions of the intelligent building or for later indirect analysis, which can provide us with an overview of the processes that take place in the building and is thus a useful tool in creating the control system as a whole. Data collection in an intelligent building can be performed either locally, where the data is stored in a repository located directly in the building, or remotely, where the data is sent for further analysis to a remote network repository.

The basic quantities most commonly measured in intelligent buildings are indoor and outdoor temperature and

relative humidity. Less frequently measured quantities mainly include concentrations of dangerous gases, such as CO or CO_2, whose monitoring allows us to analyze the state of the atmosphere in the room and to determine when the air composition in the room can be toxic to humans. In this work, temperature indoor, relative humidity indoor and CO_2 concentration indoor were recorded in five rooms of a family home for one week utilizing 5 measurement stations that were using combined Loxone temperature/ humidity/ CO_2 sensors. The rooms included: ''living room, children's room, bedroom, kitchen, and bathroom''. Technical parameters of the Loxone sensor [42] (temperature/ humidity/ CO_2 sensors) which was connected to the analog inputs directly on the Loxone Miniserver. The component are specified as follows:

- **Indoor CO_2:**Measurement Type Non-Dispersive Infrared Technology (NDIR), Measuring Range: 0… 2000 ppm, Accuracy of + 2% at 25°C and 1013 mbar < ± 50 ppm, Temperature Dependency of 2 ppm CO_2/°C, Long Term Stability 20 ppm/year, Sampling frequency Approximately 15s
- **Indoor temperature:** Accuracy at 20°C ± 0.3°C, Measuring range: 0…50°C.
- **Indoor relative humidity:** Type of measurement Capacitance, Measuring range: 0…100% RH, Accuracy at 20°C ± 3% RH.

The following steps describes the procedure of creating a project for measuring CO_2, temperature and relative humidity using the Loxone config software:

1) The project on the PC is connected to the Loxone Miniserver.
2) Furthermore, the configuration is made in the window of peripheral → Miniserver analog inputs according to the connection of the sensor. The sensor has a 0-10V output and is connected according to Figure 3.

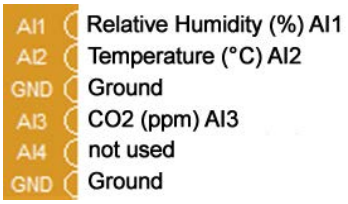

FIGURE 3. Connection of analogue inputs.

3) scaler (Program tab → Analogue tab) and 1 virtual status (Program tab → General tab) are added to each input. The result are shown in Figure 4.
4) Building properties (properties window) are set. Conversion ratios are set for the scaler according to the sensor ranges. Visualization must be enabled for virtual statuses. Next, it is necessary to set the format of the displayed value and storage of statistics with a given period. The statistics period is selected so that the values were stored more than once per minute. Furthermore, it is necessary to consider how many values will be stored since at least 10 MB of space must be retained on the memory card. To display the statistics correctly, it is also necessary to check the date and time settings on the Miniserver.

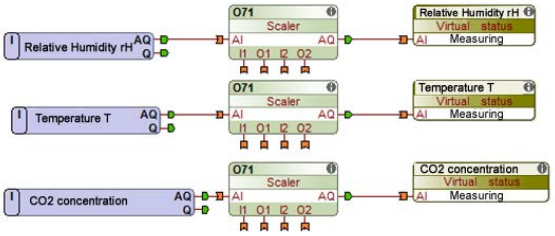

FIGURE 4. Measurement program block.

B. PREDICTIVE ANALYTICS

This section describes the Statistical and mathematical methods used to perform the development and evaluation of the predictive models. Supervised learning in neural networks is the process of estimating a function from known examples (training sets). The neural networks are non-parametric models in which the model parameters have no specific meaning with regards to the original problem [43]. The primary goal of supervised learning in neural networks is to estimate the underlying functions [43]–[46]. The Radial basis function (RBF) usually provides accurate results (mostly in regression fit problems) and high training speeds. The standard architecture of RBF artificial neural network consists of an input layer, a single hidden layer, and an output layer. The input layer associates each input variable with one independent input neuron. Therefore, the number of neurons in the input layer is equal to the number of input variables. These input neurons are fed with input values. The hidden layer contains the core logic of the network. The output layer provides a real number as a predicted value which is a scalar function of the input vector.

An RBF that consist of a single hidden layer with fixed functions in terms of size and position has a linear model. Therefore, the theory of linear models is applicable to such RBF networks. However, since the mid-'80s, some of the already familiar concepts in statistics have been renamed to neural networks [47]. When there is more than a single hidden layer or when the basic functions can be changed in size or be moved, the RBF network (model) is nonlinear. Therefore, in principle, radial functions can be used as both linear and nonlinear models; they can also be implemented as a single or multilayer configuration. However, since 1988 (since Broononlinmhead a dLowe's paper [48]), they are commonly known as single-layer networks. A typical example of a radial function includes the Gaussian function, which can be represented as the following (for scalar input) [49].

$$h(x) = e^{(}\frac{(x-c)^2}{x^2}: \tag{1}$$

If ϕ is the used function, then the center is c and the metric is R; the following equation represents the most general

formula of RBF: [43]

$$h(x) = \phi((x-c)^2 R^{-1}(x-c)) : \quad (2)$$

If x is input variable and N is the neuron count of hidden layer, then the applied RBF is formulated as:

$$a(x) = \sum_{i=0}^{N} h_i \delta(|x - c_i|) \quad (3)$$

where h, w and c stand for height, width and center of Gaussian function. $\delta(x)$ is given by:

$$\delta(x) = he^{\frac{(x-c)^2}{2w}} \quad (4)$$

For a better generalization of radial basis function networks, some nonlinear optimization is required, usually in the form of a general-purpose gradient descent [44], [50], [51]. Nevertheless, such optimizations can increase the computation cost. The RBF network implemented in this paper uses Adam as a method for stochastic optimization. It is an iterative method that optimizes the objective function. Generally, it replaces the actual gradient with an estimation. Therefore, it is considered as a stochastic approximation of gradient descent [52]. The stochastic gradient descent has become an important optimization method in machine learning [52]. The basic idea of stochastic approximation was introduced by the Robbins–Monro algorithm in the 1950s [53]. Bottou et.al call the stochastic gradient descent (SGD) algorithm ''a drastic simplification'' [54]. SGD can reduce the computational burden in big data applications [55].

Adam (Adaptive Moment Estimation) was first introduced by Kingma and Ba in 2015 [56]; the authors pointed toward the benefits of using Adam on optimization issues such as efficient computations, low memory requirements and straightforward implementation. Adam is suitable for the problems with sparse or very noisy gradients or where Hyper-parameters have intuitive interpretation and commonly need minor tuning [56]. Given parameters w^t and a loss function L^t, where t indexes the current training iteration (indexed at 0) Adam's parameter update is [56]:

$$m_w^{(t+1)} \leftarrow \beta_1 m_w^{(t)} + (1-\beta_1)\nabla_w L^{(t)} \quad (5)$$

$$v_w^{(t+1)} \leftarrow \beta_2 v_w^{(t)} + (1-\beta_2)(\nabla_w L^{(t)})^2 \quad (6)$$

$$\hat{m}_w = \frac{m_w^{(t+1)}}{1-(\beta_1)^{t+1}} \quad (7)$$

$$\hat{v}_w = \frac{v_w^{(t+1)}}{1-(\beta_2)^{t+1}} \quad (8)$$

$$w^{(t+1)} \leftarrow w^{(t)} - \eta \frac{\hat{m}_w}{\sqrt{\hat{v}_w + \epsilon}} \quad (9)$$

The performance of the trained models for unknown future inputs must be estimated. The best model is the one whose estimated prediction error is the least. Cross-valuation is a standard method for measurements of prediction errors. If the data is not scarce, the data set is divided into three parts of training, testing, validation. To avoid bias, it is better to perform this division using few different ways and then to compute an average score over different partitions [57]–[59]. Multiple models can be trained using training partition while being compared and evaluated using testing and validation partitions. To evaluate the results obtained, Mean Square Error (MSE) (formula 10) [60], Linear Correlation (LC)(formula 11) [61] and accuracy (formula 12) were used.

$$MSE = \frac{1}{n}\sum_{i-1}^{n}(y_i - \hat{y}_i)^2. \quad (10)$$

$$LC = \frac{n\sum_{i=1}^{n} y_i\hat{y}_i - \sum_{i=1}^{n} y_i \sum_{i=1}^{n} \hat{y}_i}{\sqrt{n\sum_{i=1}^{n} y_i^2 - (\sum_{i=1}^{n} y_i)^2}\sqrt{n\sum_{i=1}^{n} \hat{y}_i{}^2 (\sum_{i=1}^{n} \hat{y}_i)^2}}. \quad (11)$$

$$Accuracy = \frac{1}{n}\sum_{m=1}^{M}(1 - \frac{|y_i^{(m)} - \hat{y}_i^{(m)}|}{max_m(y_i^{(m)}) - min_m(y_i^{(m)})}). \quad (12)$$

C. ADDITIVE NOISE CANCELLATION USING LMS ADAPTIVE FILTERS

This section describes the proposed method for obtaining optimal adjustment of the LMS adaptive filter variation parameters with the Conventional LMS, the Signed-Regressor LMS algorithm, the Sign LMS algorithm, the Sign-Sign LMS algorithm of the adaptive filter. This work elaborated the current research on CO_2 concentration course processing and recognition methods, additive noise, determination of the signal-to-noise ratio, adaptive filters with the LMS algorithm, noise suppression using the adaptive filter with the LMS algorithm. The Least Mean Square (LMS) algorithm was developed by Widrow and Hoff in 1960. This algorithm is a member of the stochastic gradient algorithms [62]. The Conventional LMS algorithm is a linear adaptive filtering algorithm, which consists of two basic processes of the filtering process, which involves 13, 14, (Fig. 5) and an adaptive process(15), where w(n) is M tap – weight vector, and $w(n+1)$ is M – weight vector update [63].

$$y(n) = \sum_{i=0}^{M-1} w_i(n)x(n-i), \quad (13)$$

$$e(n) = d(n) - y(n), \quad (14)$$

$$w(n+1) = w(n) - 2\mu e(n)x(n), \quad (15)$$

The Sign LMS Algorithm is obtained from the conventional LMS recursion (15) by replacing $e(n)$ with its sign. This leads to the recursion (16) [62], [65]. The Signed-Regressor algorithm is obtained from the conventional recursion (15) by replacing the tap-input vector $x(n)$ with the vector $sign(x(n))$, where the sign function is applied to vector $x(n)$ on an element-by-element basis. The Signed-Regressor recursion is obtained from (17) [62], [65], [66]. The Sign-Sign algorithm combines the Sign and Signed-Regressor recursions, resulting in the recursion (18) [62], [65].

$$w(n+1) = w(n) + 2\mu sign(e(n))x(n), \quad (16)$$

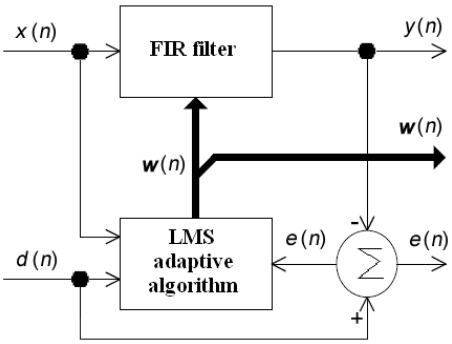

FIGURE 5. Block diagram of LMS adaptive filter [64].

$$w(n+1) = w(n) + 2\mu e(n) sign(x(n)), \quad (17)$$

$$w(n+1) = w(n) + 2\mu sign(e(n)) sign(x(n)), \quad (18)$$

To control the convergence speed and the stability of the LMS adaptive filters, it is critically important to choose an appropriate step size factor (μ) [63]. The equation (19) is used to determine the optimal value of the factor μ_{opt} [62]. $tr[R]$ is the mean sum of the diagonal elements of R or the trace of R and M_K is the misadjustment parameter [67]. The values of the misadjustment parameter are usually 10%, 20% and 30%. A value equalling 10% means that the adaptive system has an MSE only 10% greater than ζ_{min}. The dynamic time warping (DTW) is a criterion used to measure the similarities between two sequences where time and speed variation may be present. This work uses the DTW criterion to determine the suitable value for the filter length M for the LMS adaptive filter [66], [68]. The dynamic time warping (DTW) is a criterion used to measure the similarities between two sequences where time and speed variations may be present. This work uses the DTW criterion to determine the suitable value for the filter length of M for the LMS adaptive filter [66], [68]. It is critical to correctly determine the adaptive filter length of M. The short length of M results in inaccurate signal processing due to the small number of adaptive filter parameters. On the other hand, choosing a high value of M also leads to inaccurate signal processing due to the increase of estimator variance influence. Table 1 shows the length of M of the adaptive filter and distance d between the reference CO_2 concentration $d(n)$ and the output signal $y(n)$ from the LMS adaptive filter variants (first iteration), calculated by means of the draft method using the DTW criterion.

$$\mu_{opt} = \frac{M}{(1+M).tr[R]}, \quad (19)$$

The proposed method for optimal adjustment of the step size factor μ_{opt} and the filter length of M of the LMS adaptive filter was applied in the following steps [66], [69]–[71]:

1) Calculation of a step size factor μ_{opt} optimal value (19) from the input signal $x(n)$ to variations of the LMS adaptive filter ($M = 10\%$, $M = 20\%$, $M = 30\%$), (Table 1).
2) The desired signal (reference CO_2 concentration) $d(n)$ is used as reference vector P.

TABLE 1. Calculation of the length M of the adaptive filter and distance d between the reference CO_2 concentration $d(n)$ and the output signal $y(n)$ from the LMS adaptive filter variants (first iteration), calculated by means of the draft method using the DTW criterion (simulated in MATLAB).

LMS AF Type	SIGN	SIGN - SIGN	SIGN - REG
M= 10%	$\mu_1 = 3.91 \times 10^{-3}$; $M = 5$	$\mu_1 = 3.91 \times 10^{-3}$; $M = 2$	$\mu_1 = 3.91 \times 10^{-2}$; $M = 26$
M= 20%	$\mu_2 = 7.17 \times 10^{-2}$; $M = 3$	$\mu_2 = 7.16 \times 10^{-2}$; $M = 2$	$\mu_2 = 7.16 \times 10^{-2}$; $M = 48$
M= 30%	$\mu_3 = 9.92 \times 10^{-3}$; $M = 2$	$\mu_3 = 9.92 \times 10^{-3}$; $M = 2$	$\mu_3 = 9.92 \times 10^{-2}$; $M = 44$

3) The output signal $y(n)$ was selected as test vector O.
4) Next, the distance d between the courses $d(n)$ and $y(n)$ was calculated for the settings of the filter lengths of M of the LMS adaptive filter variations in interval 1 to 150 (Figure 6).
5) The same procedure was used to calculate the optimal filter length of M of other variations of the LMS adaptive filter (the Signed, the Signed-Regressor and the Signed-Signed LMS adaptive filter). As an example, the Signed-Regressor LMS algorithm was chosen, wherein the filter length of $M = 26$, for minimum distance $d = 0.07927$ (Figure 6), (Table 1) between two compared signals $d(n)$ and $y(n)$ ($\mu_1 = 3.907 \times 10^{-3}$) was calculated.

D. SOFTWARE DEVELOPMENT

Python is an interpreted, general-purpose and high-level programming language that aims to assist programmers to write logical and clear code [72]. Python comprises maps, filters, and reduces functions such as sets, expression generators, list comprehensions, and dictionaries [73]. Python is often referred to as a ''batteries included'' language because of its relevantly comprehensive standard library [74]–[77]. However, Python was designed to be highly extensible rather than including all of its functionality into its core. In the last few years, Python has only become popular for symbolic computing [76]. All calculations in this paper were performed using the Tensorflow library which is a symbolic math library that is commonly used for machine learning applications such as neural networks. The main advantage of employing Tensorflow is parallel computation; computational tasks can be easily divided between the machine's Processing cores (Central Processing Unit (CPU), Graphical Processing Unit (GPU) and Tensor Processing Unit (TPU)). According to the TensorBoard software, 95% of the network calculations are compatible with TPU [78]. Tensorflow is ideal for GPU computing due to the creation of an algorithm graph that provides the possibility of parallel computation [78].

The data were imported to the Python environment using Pandas. Pandas is a free software which is developed for the Python environment. It provides data structures and operations for manipulating numerical tables and time series. As explained earlier, partitioning is an important step for model evaluation and selection. Using the panda library

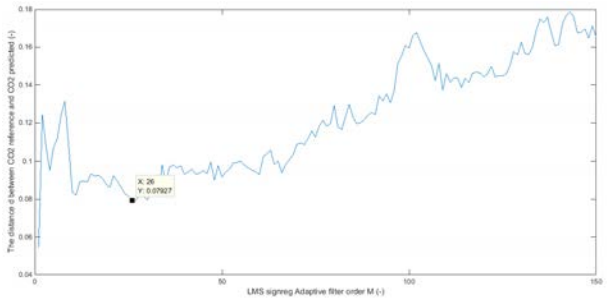

FIGURE 6. Calculation of the length of $M = 26$ of the Signed-Regressor LMS Adaptive filter algorithm and distance $d = 0.07927$ (Table 1) between CO_2 reference and CO_2 predicted course in the Kitchen.

(function sample), the data set was partitioned into three sets of training (40%), testing (30%), and validation (30%). The neural network (RBF) implementation was performed using the Keras library. The Keras library is an open-source neural-network library that enables fast implementation of deep neural networks. Keras is built on the TensorFlow library and provides a cleaner and simpler API for building neural network models [78]–[80]. However, Keras doesn't include the RBF in its framework. Therefore, the RBF ANN had to be implemented as a new layer within the Keras framework. The two variables of indoor temperature and relative humidity were chosen as predictors. Therefore, the input layer of theRBF network was configured as a two-dimensional vector (Figure 7). The input layer forms a matrix with two rows (indoor temperature and relative humidity) and n columns, where n is the batch size (number of CO_2 concentration level predictions). The input layer propagates these values to the hidden layer. The network employed a single-hidden layer that consists of different Gaussians (with Gaussian parameters of height and spread). The RBF layer (hidden layer) affects the height of the Gaussian (the output of the function with a given argument) and propagates the calculated values to the output layer. The range of 5 to 600 was selected as the neurons count in the hidden layer. The Output layer multiplies the output of the previous, Hidden layer, with the vector of weights (W) and represented it in a scalar form.

IV. EXPERIMENTS AND RESULTS

The experiments were performed in a smart home using Loxone technology. The sensors were placed in five different locations (bedroom, children's room, living room, bathroom, and kitchen) within the smart home to ensure the integrity and validity of the results. The external sources of heat and humidity often influence the measurement in locations such as the kitchen and bathroom. This influence was previously assumed to create a significant challenge for accurate predictions of the CO_2 concentration waveform. A total data interval of nine days (22nd to 31st December 2019) was recorded. For accuracy comparison, this interval was divided into two one-day-long (2018/12/22 00:00 to 2018/12/22 23:59

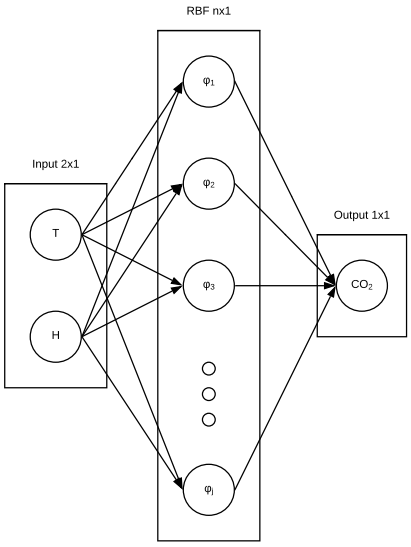

FIGURE 7. Model of the implemented RBF neural network.

and 2018/12/23 00:00 to 2018/12/23 23:59), one-week-long (2018/12/22 00:00 to 2018/12/29 23:59) and ten-day-long intervals (2018/12/22 00:00 to 2018/12/31 23:59). Table 2 shows the 20 different data sets used to train and validate the proposed solution.

A. CHILDREN'S ROOM

The first experimental location was the children's room. With a few exceptions, the overall trend of the results obtained showed accuracy improvements with the increase in the number of neurons. However, the average of these improvements was insignificant. Table 3 shows a slight drop in average accuracy with the number of the hidden layer neurons count larger than 400. The highest accuracy (96.0%) was obtained from a model with the 600 hidden layer neurons count and the C1 training interval (22nd December 2018/12/22 00:00 to 2018/12/22 23:59). Further investigation suggested that the models with shorter training interval lengths (smaller data sets) achieved better accuracy (up to 95%). However, the interval length of ten days showed slightly better characteristics in comparison with the seven-day interval. This could be an indication of overfitting reduction caused by the inclusion of sample data sets with a slightly different correlation between the predictors and the predictions. In the comparison of the reference CO_2 and the predicted course of CO_2 filtered using the signed-regressor LMS algorithm of the adaptive filter (Figure 8) in the children's room, it can unequivocally be said that there was a noticeable improvement in the accuracy.

B. BEDROOM

The analysis performed on the results obtained from bedroom data sets showed a slight oscillation of accuracy with

TABLE 2. Training Data sets.

Interval (Dec)	Childeren's room	Bedroom	living room	Kitchen	Bathroom
22^{nd}	C1	B1	L1	K1	W1
23^{rd}	C2	B2	L2	K2	W2
22^{nd}-29^{th}	C3	B3	L3	K3	W3
22^{nd}-31^{st}	C4	B4	L4	K4	W4

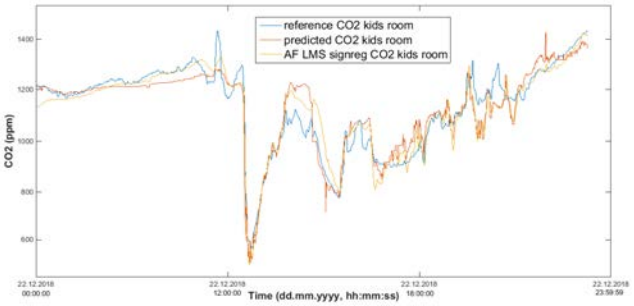

FIGURE 8. Blue: reference CO_2 waveform (ppm), black: Predicted CO_2 waveform (ppm). red: fileterd prediction using signed – regressor LMS adaptive filtration ($\mu = 2.2 \times 10^{-2}$ and $M = 5$), (children room day long training interval of 22.12.2018).

regards to the hidden layer neuron count. Table 5 clearly shows that the oscillation of average accuracy is insignificant. Therefore, the number of neurons does not significantly impact the results. The highest accuracy (95.5%) was achieved by the model with the 500 hidden layer neuron count and the training interval of B1 (22^{nd} December 2018/12/22 00:00 to 2018/12/22 23:59). Overall, the accuracy of the one-day-long intervals was significantly higher than the longer intervals (seven-day-long and ten-day-long). Table 5 additionally shows that, depending on the interval lengths, the accuracy may vary up to the significant value of 10%. Figure 9 compares the reference CO_2 and the predicted course of CO_2 filtered using the signed-regressor LMS algorithm of the adaptive filter. This comparison demonstrates the significance of improvement in prediction accuracy.

C. LIVING ROOM

After performing the analysis on living room data sets, it became apparent that only the ten-day-long interval showed a constant increase in accuracy with an increase of neurons in the hidden layer. Few fluctuations could be observed across the accuracy of the other data sets (concerning the number of neurons in the hidden layer). With data set L1 (22^{nd} December 2018/12/22 00:00 to 2018/12/22 23:59), the accuracy of the models with 500 and 600 neurons in their hidden layers drops, which could be caused by overfitting. The highest accuracy (93.2%) was obtained from the model with 500 neurons (in the hidden layer) and the training interval L1. Table 7 shows the average of each model (examined by different intervals). It can be observed that the number of neurons does not significantly impact the accuracy. On the other hand, Table 8 shows that shorter intervals (one-day-long) are significantly more accurate. The waveform of the predicted course of CO_2 showed significant improvements after being filtered using the signed-regressor LMS algorithm of the adaptive filter (Figure 10).

D. KITCHEN

In the kitchen, the CO_2 waveform appears to be less dependent on the number of people. A single person cooking may increase humidity, temperature, and CO_2 significantly. The analysis showed no apparent dependency between the accuracy and the number of neurons. However, in all particular

TABLE 3. Children's room analysis, average accuracy of the developed models using different intervals.

Neuron Count	Accuracy(%)	Linear Correlation(-)	MSE(-)
5	90.087	0.813	7.881×10^{-3}
10	90.095	0.817	7.760×10^{-3}
25	90.561	0.836	7.091×10^{-3}
50	90.664	0.838	7.064×10^{-3}
75	90.731	0.846	6.850×10^{-3}
100	90.839	0.847	6.793×10^{-3}
200	90.839	0.848	6.695×10^{-3}
300	91.073	0.853	6.638×10^{-3}
400	91.227	0.854	6.456×10^{-3}
500	91.087	0.857	6.482×10^{-3}
600	91.168	0.855	6.449×10^{-3}

TABLE 4. Children's room analysis, Average of each interval using different models.

Interval	Accuracy(%)	Linear Correlation(-)	MSE(-)
C1	95.738	0.927	2.241×10^{-3}
C2	95.068	0.932	1.988×10^{-3}
C3	84.382	0.697	1.373×10^{-2}
C4	87.857	0.812	9.737×10^{-3}

TABLE 5. Bedroom analysis, average accuracy of the developed models using different intervals.

Neuron Count	Accuracy(%)	Linear Correlation(-)	MSE(-)
5	88.198	0.789	1.036×10^{-2}
10	88.087	0.797	1.002×10^{-2}
25	89.044	0.819	9.174×10^{-3}
50	89.101	0.822	9.091×10^{-3}
75	88.945	0.821	9.082×10^{-3}
100	89.081	0.823	8.979×10^{-3}
200	88.965	0.824	9.066×10^{-3}
300	88.903	0.824	8.960×10^{-3}
400	89.269	0.825	8.993×10^{-3}
500	88.979	0.827	8.884×10^{-3}
600	89.248	0.827	8.868×10^{-3}

TABLE 6. Bedroom analysis, Average of each interval using different models.

Interval	Accuracy(%)	Linear Correlation(-)	MSE(-)
B1	95.236	0.932	3.155×10^{-3}
B2	93.181	0.907	2.717×10^{-3}
B3	83.273	0.670	1.657×10^{-2}
B4	83.881	0.763	1.446×10^{-2}

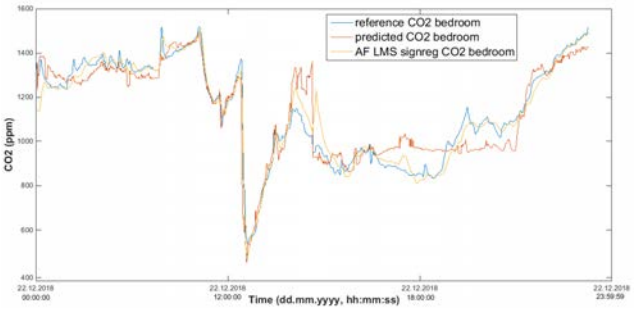

FIGURE 9. Blue: reference CO_2 waveform (ppm), black: Predicted CO_2 waveform (ppm). red: fileterd prediction using signed – regressor LMS adaptive filtration ($\mu = 1.66 \times 10^{-2}$ and $M = 26$), (bedroom day long training interval of 22.12.2018).

data sets (interval), the difference between the lowest and highest accuracy is negligible. Table 9 further supports the observation of relatively constant accuracy across all models (different number of neurons in the hidden layer). Table 9 shows significantly more accurate results for shorter intervals (one-day-long). The highest accuracy (95.6%) was obtained by the model with 300 neurons in the hidden layer and the K1 training data set (22nd December 2018/12/22 00:00 to 2018/12/22 23:59). The waveform of the predicted course of CO_2 showed significant improvements after being filtered using the signed-regressor LMS algorithm of the adaptive filter (Figure 11).

E. BATHROOM

Similarly to the kitchen, external sources of heat and humidity are also present in bathrooms. The data collected showed a consistent pattern caused by the single-purpose nature of bathrooms. This should improve the accuracy of the predictions. The highest accuracy (96.7%) was obtained from the training data set W1 (22nd December 2018/12/22 00:00 to 2018/12/22 23:59) and the model with the 600 hidden layer neuron count. Except for the model with 5 neurons in the hidden layer (accuracy of 93.3), all of the trained models with this interval resulted in an accuracy above 96.4%. Similarly, the result from the data set W2 (23rd December 2018/12/23 00:00 to 2018/12/23 23:59) were also accurate (accuracy range: 94.5% to 95.6%). Following the trend of every

TABLE 8. Living room analysis, Average of each interval using different models.

Interval	Accuracy(%)	Linear Correlation(-)	MSE(-)
L1	92.698	0.807	3.671×10^{-3}
L2	92.854	0.893	3.765×10^{-3}
L3	82.758	0.652	1.664×10^{-2}
L4	83.614	0.690	1.496×10^{-2}

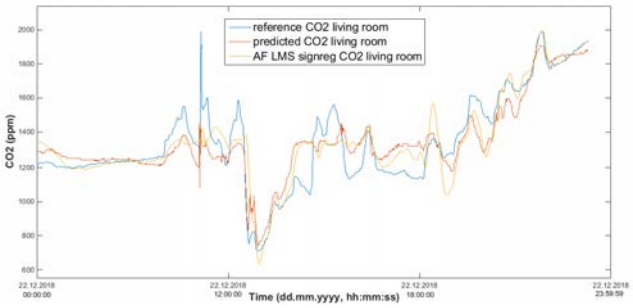

FIGURE 10. Blue: reference CO_2 waveform (ppm), black: Predicted CO_2 waveform (ppm). red: filtered prediction using signed – regressor LMS adaptive filtration ($\mu = 2.56 \times 10^{-2}$ and $M = 26$), (living room day long training interval of 22.12.2018).

experiment performed earlier, the larger data sets (seven-day-long and ten-day- long) resulted in reduced accuracy (accuracy range: 79.5% to 82.9%). Table 12 shows up to 15% difference in average accuracy of these intervals. With a few exceptions, the overall trend of the results suggested improvement in accuracy with the increase of neurons. However, these improvements can be considered insignificant. Table 12 further reflects these observations. Figure 12 shows the accuracy improvements obtained using the signed-regressor LMS adaptive filter in the bathroom analysis.

V. DISCUSSION

This article describes the procedure of the of CO_2 concentration prediction from the measured indoor relative humidity and temperature and indoor (measured using Loxone). Due to the high prediction accuracy and short training time, ANN RBF was selected as a statistical method to perform the predictions. By observing all the experiments performed, it became apparent that the number of neurons in the hidden layer does not significantly impact the accuracy. The analysis

TABLE 7. Living room analysis, average accuracy of the developed models using different intervals.

Neuron Count	Accuracy(%)	Linear Correlation(-)	MSE(-)
5	87.273	0.732	1.052×10^{-2}
10	87.259	0.731	1.061×10^{-2}
25	87.969	0.752	9.808×10^{-3}
50	88.438	0.760	9.663×10^{-3}
75	88.241	0.761	9.632×10^{-3}
100	88.056	0.762	9.666×10^{-3}
200	88.013	0.768	9.743×10^{-3}
300	88.310	0.769	9.388×10^{-3}
400	87.674	0.772	9.607×10^{-3}
500	88.252	0.777	9.432×10^{-3}
600	88.307	0.777	9.277×10^{-3}

TABLE 9. Kitchen analysis,average accuracy of the developed models using different intervals.

Neuron Count	Accuracy(%)	Linear Correlation(-)	MSE(-)
5	86.000	0.606	1.248×10^{-2}
10	87.023	0.675	1.134×10^{-2}
25	87.459	0.711	1.064×10^{-2}
50	87.162	0.708	1.082×10^{-2}
75	87.440	0.707	1.066×10^{-2}
100	87.185	0.713	1.074×10^{-2}
200	87.808	0.718	1.047×10^{-2}
300	87.937	0.721	1.032×10^{-2}
400	88.095	0.721	1.055×10^{-2}
500	87.663	0.722	1.027×10^{-2}
600	87.401	0.723	1.046×10^{-2}

TABLE 10. Kitchen analysis, Average of each interval using different models.

Interval	Accuracy(%)	Linear Correlation(-)	MSE(-)
K1	94.810	0.835	2.343×10^{-3}
K2	91.377	0.782	7.022×10^{-3}
K3	81.505	0.499	1.710×10^{-2}
K4	81.827	0.709	1.671×10^{-2}

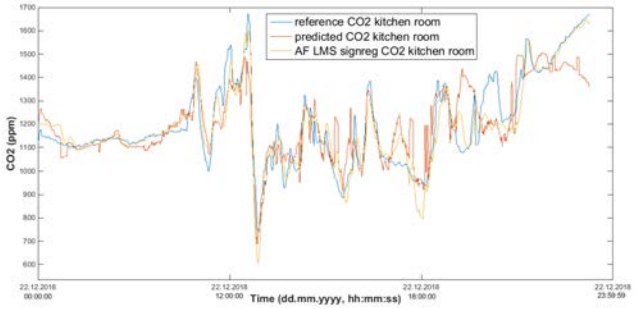

FIGURE 11. Blue: reference CO_2 waveform (ppm), black: Predicted CO_2 waveform (ppm). red: filtered prediction using signed – regressor LMS adaptive filtration ($\mu = 3,907 \times 10^{-2}$ and $M = 26$) (kitchen day long training interval of 22.12.2018).

TABLE 11. Bathroom analysis, Average accuracy of the developed models using different intervals.

Neuron Count	Accuracy(%)	Linear Correlation(-)	MSE(-)
5	87.084	0.675	1.177×10^{-2}
10	88.237	0.755	1.077×10^{-2}
25	88.618	0.777	1.012×10^{-2}
50	88.791	0.780	1.010×10^{-2}
75	88.699	0.784	1.009×10^{-2}
100	88.744	0.782	1.009×10^{-2}
200	88.867	0.793	9.864×10^{-3}
300	88.929	0.792	9.693×10^{-3}
400	89.341	0.794	9.658×10^{-3}
500	89.217	0.795	9.655×10^{-3}
600	89.076	0.797	9.715×10^{-3}

TABLE 12. Bathroom analysis, Average of each interval using different models.

Interval	Accuracy(%)	Linear Correlation(-)	MSE(-)
W1	96.364	0.898	1.402×10^{-3}
W2	94.941	0.944	1.935×10^{-3}
W3	81.838	0.600	1.801×10^{-2}
W4	81.622	0.658	1.921×10^{-2}

showed that in some cases (such as children's room with the interval of (2018/12/22 00:00 to 2018/12/22 23:59) the difference between the accuracy of the models with 5 and 600 neurons in the hidden layer can be as insignificant as 0.1%. This could be a direct result of low dimension data sets (total of 3 variables). The highest accuracy (97%) was obtained in the bathroom with the interval of 22nd December. The training interval of 22nd December resulted in the most accurate results across all the locations within the smart home. These results were closely followed by the training interval of 23rd December. On the other hand, the week-long and ten-day-long intervals showed significantly lower accuracy.

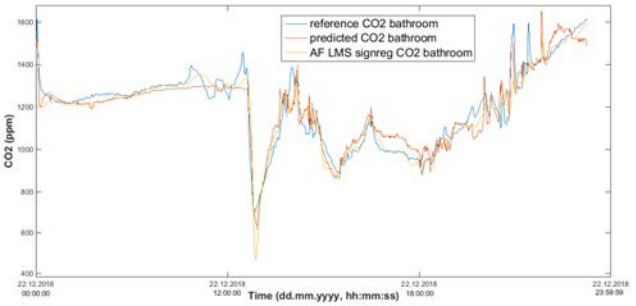

FIGURE 12. Blue: reference CO_2 waveform (ppm), black: Predicted CO_2 waveform (ppm). red: filtered prediction using signed – regressor LMS adaptive filtration ($\mu = 2.78 \times 10^{-2}$ and $M = 10$) of prediction waveform using RBF NN (black), (bathroom day long training interval of 22.12.2018).

To accurately predict the CO_2 concentration levels, a newly designed noise suppression method was used. This method investigated the optimal adjustment of the values of the individual parameters of the adaptive filter with the Sign, Sign-Sign and Sign-Regressor LMS Algorithms. The method first chooses a suitable LMS algorithm structure for the adaptive filter and conducts a simulation in the MATLAB Software. Next, to meet the conditions that are ensuring convergence and stability of the LMS adaptive filter, the optimal value of the parameter was calculated from the input signal $x(n)$ (predicted CO_2) and reference signal $d(n)$ (measured CO_2). Lastly, for optimal adjustment of the LMS adaptive filter, M order value was calculated. Figure 6 displays the plotted optimal value of the order of M obtained by calculation. The optimal adaptive filter structure was the Signed-Regressor LMS Algorithm with a step size of $\mu = 3,907 \times 10^{-2}$ and an order of the adaptive filter of $M = 26$ (Figure 6). Figures 8, 9, 10, 11 and 12 clearly show the improvements of the predicted CO_2 concentration waveform with the application of the additive noise suppression method introduced.

This work addresses many of the previous concerns, such as the possibility of measurements and predictions in locations, such as bathroom and kitchen, the effects of interval lengths and the number of neurons, and the optimal noise suppression method. However, there are a few more areas to explore. As an example, the possibility of employing support vector machines (SVM) or fuzzy systems, as an alternative solution to the ANN, may increase the chance of developing a universal prediction model by focusing on a border picture.

VI. CONCLUSION

The article describes a proposal of a newly designed indirect method for detecting occupancy of monitored areas in intelligent buildings using the prediction of the CO_2 concentration waveform from operational measurement of non-electrical quantities (temperature indoor, relative humidity indoor) using of artificial neural network (ANN) based on the Radial Basis Function (RBF), developed in the Python environment. In order to make the newly proposed CO_2 prediction method

more accurate, another newly designed method was used to optimally adjust the parameters (filter length M and step size parameter μ) of the adaptive filter with variations in the LMS algorithm in the additive noise suppression application. Based on the experiments conducted from December 22, 2018, to December 31, 2018, in five selected rooms of a real family home: ''living room, children's room, bedroom, kitchen, and bathroom''. It can be stated that the newly devised method is fairly accurate even for the areas with increased relative humidity formation due to human activity, such as cooking (kitchen) or showering (bathroom). In the presented experiments, the accuracy of the introduced method exceeded 95%. The achieved results shows a promising path for prediction of CO2 and low cost indirect occupancy monitoring. The author's future work will be to use the newly proposed method in practical implementations for HVAC control in an intelligent building within an IoT platform and for recognition of daily living activities of seniors and disabled in Smart Home Care.

REFERENCES

[1] M. A. Zehir, A. Batman, M. A. Sonmez, A. Font, D. Tsiamitros, D. Stimoniaris, T. Kollatou, M. Bagriyanik, A. Ozdemir, and E. Dialynas, ''Development of a field data-based virtual test bed for microgrid integration of building automation technologies,'' in *Proc. 9th Int. Conf. Electr. Electron. Eng. (ELECO)*, Nov. 2015, pp. 51–55.

[2] D. Stimoniaris, T. Kollatou, D. Tsiamitros, K. Gavros, V. Kikis, S. Asimonis, M. A. Zehir, A. Batman, M. Bagriyanik, A. Ozdemir, and E. Dialynas, ''Cooperation scheme between KNX and a microgrid control system for enhanced demand-side management,'' in *Proc. 9th Int. Conf. Electr. Electron. Eng. (ELECO)*, Nov. 2015, pp. 46–50.

[3] M. Massoth, R. Acker, N. Buchmann, T. Fugmann, C. Knoell, and M. Porzelt, ''Ubiquitous smart grid control solution based on a next generation network as integration platform,'' *Energy*, pp. 173–178, 2011.

[4] E. Temuulen, G. Hasegawa, Y. Tarutani, K. Matsuda, and M. Matsuoka, ''Large-scale ASP-based HEMS utilizing interactive web technologies,'' in *Proc. IEEE Int. Conf. Smart Grid Commun. (SmartGridComm)*, Nov. 2015, pp. 798–803.

[5] D. Szendrei, T. Teich, S. Franke, and M. Schrader, ''Hydraulic balance in smart homes-using the KNX-standard for performing balanced heating conditions in dynamic load situations,'' in *Proc. ICINCO*, 2011, pp. 381–386.

[6] J. Vanus, T. Weiper, R. Martinek, J. Nedoma, M. Fajkus, L. Koval, and R. Hrbac, ''Assessment of the quality of speech signal processing within voice control of operational-technical functions in the smart home by means of the PESQ algorithm,'' *IFAC-PapersOnLine*, vol. 51, no. 6, pp. 202–207, 2018.

[7] J. Vanus, M. Smolon, R. Martinek, J. Koziorek, J. Zidek, and P. Bilik, ''Testing of the voice communication in smart home care,'' *Hum.-Centric Comput. Inf. Sci.*, vol. 5, no. 1, p. 15, Dec. 2015.

[8] G. Wang, S. Lu, D. Pang, and R. Wu, ''The design of smart home gateway based on KNX bus,'' in *Proc. Int. Conf. Logistics, Eng., Manage. Comput. Sci.*, 2015, pp. 1225–1228.

[9] M. Markiewicz, ''An event-based language for simplified definition of home automation control routines,'' in *Proc. Int. Conf. Event-Based Control, Commun., Signal Process. (EBCCSP)*, Jun. 2015, pp. 1–6.

[10] J. Vanus, J. Belesova, R. Martinek, J. Nedoma, M. Fajkus, P. Bilik, and J. Zidek, ''Monitoring of the daily living activities in smart home care,'' *Hum.-Centric Comput. Inf. Sci.*, vol. 7, no. 1, p. 30, Dec. 2017.

[11] J. Vanus, M. Cerny, and J. Koziorek, ''The proposal of the smart home care solution with KNX components,'' in *Proc. 38th Int. Conf. Telecommun. Signal Process. (TSP)*, Jul. 2015, pp. 1–5.

[12] T. Novak, J. Vanus, J. Sumpich, J. Koziorek, K. Sokansky, and R. Hrbac, ''Possibility to achieve the energy savings by the light control in smart home,'' in *Proc. 7th Int. Sci. Symp. Elect. Power Eng. (Elektroenergetika)*, 2013, pp. 260–263.

[13] J. Vanus, P. Valicek, T. Novak, R. Martinek, P. Bilik, and J. Zidek, ''Utilization of regression analysis to increase the control accuracy of dimmer lighting systems in the smart home,'' *IFAC-PapersOnLine*, vol. 49, no. 25, pp. 517–522, 2016.

[14] P. Valicek, T. Novak, J. Vanus, K. Sokansky, and R. Martinek, ''Measurement of illuminance of interior lighting system automatically dimmed to the constant level depending on daylight,'' in *Proc. IEEE 16th Int. Conf. Environ. Electr. Eng. (EEEIC)*, Jun. 2016, pp. 1–5.

[15] J. Song, S. C. Sierra, J. C. Rodriguez, J. M. Perandones, G. Del Campo Jimenez, J. O. Bujan, R. M. Garcia, and A. S. Galdon, ''Parameter-based mechanism for unifying user interaction, applications and communication protocols,'' in *Proc. 2nd Int. Conf. Artif. Intell., Modelling Simulation*, Nov. 2014, pp. 131–136.

[16] J. Petnik and J. Vanus, ''Design of smart home implementation within IoT with natural language interface,'' *IFAC-PapersOnLine*, vol. 51, no. 6, pp. 174–179, 2018.

[17] G. De Luca, P. Lillo, L. Mainetti, V. Mighali, L. Patrono, and I. Sergi, ''The use of NFC and Android technologies to enable a KNX-based smart home,'' in *Proc. 21st Int. Conf. Softw., Telecommun. Comput. Netw. (SoftCOM)*, Sep. 2013, pp. 1–7.

[18] S. Ilieva, A. Penchev, and D. Petrova-Antonova, ''Internet of Things framework for smart home building,'' in *Proc. Int. Conf. Digit. Transf. Global Soc.* Cham, Switzerland: Springer, 2016, pp. 450–462.

[19] L. Mainetti, V. Mighali, and L. Patrono, ''An Android multi-protocol application for heterogeneous building automation systems,'' in *Proc. 22nd Int. Conf. Softw., Telecommun. Comput. Netw. (SoftCOM)*, Sep. 2014, pp. 121–127.

[20] S. Oudji, S. Courreges, J.-N. Paillard, V. Meghdadi, and P. Michel, ''Radio interference challenges in a multiprotocol compact RF hardware platform for home and building automation applications,'' *Int. J. Commun. Syst.*, vol. 31, no. 8, p. e3535, May 2018.

[21] E. Leite, L. Varela, V. F. Pires, F. D. Cardoso, A. J. Pires, and J. F. Martins, ''A ZigBee wireless domotic system with Bluetooth interface,'' in *Proc. 40th Annu. Conf. IEEE Ind. Electron. Soc. (IECON)*, Oct. 2014, pp. 2506–2511.

[22] N. Langhammer and R. Kays, ''Performance evaluation of wireless home automation networks in indoor scenarios,'' *IEEE Trans. Smart Grid*, vol. 3, no. 4, pp. 2252–2261, Dec. 2012.

[23] M. Jung, J. Weidinger, W. Kastner, and A. Olivieri, ''Building automation and smart cities: An integration approach based on a service-oriented architecture,'' in *Proc. 27th Int. Conf. Adv. Inf. Netw. Appl. Workshops*, Mar. 2013, pp. 1361–1367.

[24] O. Arnold, L. Kirsch, and A. Schulz, ''An interactive concierge for independent living,'' in *Proc. IEEE 3rd Global Conf. Consum. Electron. (GCCE)*, Oct. 2014, pp. 59–62.

[25] C. Brennan, G. W. Taylor, and P. Spachos, ''Designing learned CO_2-based occupancy estimation in smart buildings,'' *IET Wireless Sensor Syst.*, vol. 8, no. 6, pp. 249–255, Dec. 2018.

[26] B. Khazaei, A. Shiehbeigi, and A. R. H. M. A. Kani, ''Modeling indoor air carbon dioxide concentration using artificial neural network,'' *Int. J. Environ. Sci. Technol.*, vol. 16, no. 2, pp. 729–736, Feb. 2019.

[27] J. Skön, M. Johansson, M. Raatikainen, K. Leiviskä, and M. Kolehmainen, ''Modelling indoor air carbon dioxide (CO_2) concentration using neural network,'' *Methods*, vol. 14, no. 15, p. 16, 2012.

[28] J. Vanus, R. Martinek, P. Bilik, J. Zidek, P. Dohnalek, and P. Gajdos, ''New method for accurate prediction of CO_2 in the smart home,'' in *Proc. IEEE Int. Instrum. Meas. Technol. Conf.*, May 2016, pp. 1–5.

[29] J. Vanus, J. Machac, R. Martinek, P. Bilik, J. Zidek, J. Nedoma, and M. Fajkus, ''The design of an indirect method for the human presence monitoring in the intelligent building,'' *Hum.-Centric Comput. Inf. Sci.*, vol. 8, no. 1, p. 28, Dec. 2018.

[30] J. Vanus, J. Kubicek, O. M. Gorjani, and J. Koziorek, ''Using the IBM SPSS SW tool with wavelet transformation for CO_2 prediction within IoT in smart home care,'' *Sensors*, vol. 19, no. 6, p. 1407, Mar. 2019.

[31] *HVAC Room Transmitter and Switches for CO_2, Relative Humidity and Temperature*, Loxone, Kollerschlag, Austria.

[32] V. Aragon, S. Gauthier, P. Warren, P. A. B. James, and B. Anderson, ''Developing English domestic occupancy profiles,'' *Building Res. Inf.*, vol. 47, no. 4, pp. 375–393, May 2019.

[33] Z. Chen, C. Jiang, and L. Xie, ''Building occupancy estimation and detection: A review,'' *Energy Buildings*, vol. 169, pp. 260–270, Jun. 2018.

[34] S. Azizi, G. Nair, R. Rabiee, and T. Olofsson, ''Application of Internet of Things in academic buildings for space use efficiency using occupancy and booking data,'' *Building Environ.*, vol. 186, Dec. 2020, Art. no. 107355.

[35] V. Becker and W. Kleiminger, "Exploring zero-training algorithms for occupancy detection based on smart meter measurements," *Comput. Sci.-Res. Develop.*, vol. 33, nos. 1–2, pp. 25–36, Feb. 2018.
[36] L. M. Candanedo, V. Feldheim, and D. Deramaix, "A methodology based on hidden Markov models for occupancy detection and a case study in a low energy residential building," *Energy Buildings*, vol. 148, pp. 327–341, Aug. 2017.
[37] A. Capozzoli, M. S. Piscitelli, A. Gorrino, I. Ballarini, and V. Corrado, "Data analytics for occupancy pattern learning to reduce the energy consumption of HVAC systems in office buildings," *Sustain. Cities Soc.*, vol. 35, pp. 191–208, Nov. 2017.
[38] J. Dong, C. Winstead, J. Nutaro, and T. Kuruganti, "Occupancy-based HVAC control with short-term occupancy prediction algorithms for energy-efficient buildings," *Energies*, vol. 11, no. 9, p. 2427, Sep. 2018.
[39] O. M. Gorjani, P. Bilik, and J. Vanus, "Application of optimized deterministic methods in long-term power quality," in *Proc. 20th Int. Sci. Conf. Electr. Power Eng. (EPE)*, May 2019, pp. 1–5.
[40] J. Vanus, O. M. Gorjani, and P. Bilik, "Novel proposal for prediction of CO_2 course and occupancy recognition in intelligent buildings within IoT," *Energies*, vol. 12, no. 23, p. 4541, Nov. 2019.
[41] *Loxone*, Loxone, Kollerschlag, Austria.
[42] *HVAC Room Transmitter and Switches for CO_2, Relative Humidity and Temperature*, Loxone, Kollerschlag, Austria.
[43] R. N. Bracewell and R. N. Bracewell, *The Fourier Transform and Its Applications*, vol. 31999. New York, NY, USA: McGraw-Hill, 1986.
[44] N. B. Karayiannis, "Reformulated radial basis neural networks trained by gradient descent," *IEEE Trans. Neural Netw.*, vol. 10, no. 3, pp. 657–671, May 1999.
[45] J. Fan, "Design-adaptive nonparametric regression," *J. Amer. Stat. Assoc.*, vol. 87, no. 420, pp. 998–1004, Dec. 1992.
[46] D. F. Specht, "A general regression neural network," *IEEE Trans. Neural Netw.*, vol. 2, no. 6, pp. 568–576, Nov. 1991.
[47] W. S. Sarle, "Neural networks and statistical models," Tech. Rep., 1994.
[48] D. S. Broomhead and D. Lowe, "Radial basis functions, multi-variable functional interpolation and adaptive networks," Royal Signals Radar Establishment Malvern United Kingdom, Tech. Rep., 1988.
[49] M. J. Orr *et al.*, "Introduction to radial basis function networks," Tech. Rep., 1996.
[50] D. Simon, "Training radial basis neural networks with the extended Kalman filter," *Neurocomputing*, vol. 48, nos. 1–4, pp. 455–475, Oct. 2002.
[51] S. Chen, C. F. N. Cowan, and P. M. Grant, "Orthogonal least squares learning algorithm for radial basis function networks," *IEEE Trans. Neural Netw.*, vol. 2, no. 2, pp. 302–309, Mar. 1991.
[52] M. Taddy, *Business Data Science: Combining Machine Learning and Economics to Optimize, Automate, and Accelerate Business Decisions*. New York, NY, USA: McGraw-Hill, 2019.
[53] S. Mei, A. Montanari, and P.-M. Nguyen, "A mean field view of the landscape of two-layer neural networks," *Proc. Nat. Acad. Sci. USA*, vol. 115, no. 33, pp. E7665–E7671, Aug. 2018.
[54] L. Bottou, "Large-scale machine learning with stochastic gradient descent," in *Proc. COMPSTAT*. Springer, 2010, pp. 177–186.
[55] L. Bottou and O. Bousquet, "The tradeoffs of large scale learning," in *Proc. Adv. Neural Inf. Process. Syst.*, 2008, pp. 161–168.
[56] D. P. Kingma and J. Ba, "Adam: A method for stochastic optimization," 2014, *arXiv:1412.6980*.
[57] R. Kohavi, "A study of cross-validation and bootstrap for accuracy estimation and model selection," in *Proc. IJCAI*, Montreal, QC, Canada, vol. 14, 1995, pp. 1137–1145.
[58] A. Krogh and J. Vedelsby, "Neural network ensembles, cross validation, and active learning," in *Proc. Adv. Neural Inf. Process. Syst.*, 1995, pp. 231–238.
[59] G. H. Golub, M. Heath, and G. Wahba, "Generalized cross-validation as a method for choosing a good ridge parameter," *Technometrics*, vol. 21, no. 2, pp. 215–223, May 1979.
[60] E. L. Lehmann and G. Casella, *Theory of Point Estimation*. Springer, 2006.
[61] Y. Ijiri, "The linear aggregation coefficient as the dual of the linear correlation coefficient," *Econometrica, J. Econ. Soc.*, pp. 252–259, 1968.
[62] B. Farhang-Boroujeny, *Adaptive Filters: Theory and Applications*. Hoboken, NJ, USA: Wiley, 2013.
[63] A. D. Poularikas and Z. M. Ramadan, *Adaptive Filtering Primer With MATLAB*. Boca Raton, FL, USA: CRC Press, 2017.
[64] J. Jan., "Cislicova filtrace, analyza a restaurace signalu, nakladatelstvi vutium, brno," Tech. Rep., 2002, pp. 287–308.
[65] R. Chassaing, *Digital Signal Processing and Applications With the C6713 and C6416 DSK*, vol. 16. Hoboken, NJ, USA: Wiley, 2004.
[66] J. Vanus and V. Styskala, "Application of variations of the LMS adaptive filter for voice communications with control system," Tech. Rep., 2011.
[67] C. V. Jakowatz, D. E. Wahl, P. H. Eichel, D. C. Ghiglia, and P. A. Thompson, *Spotlight-Mode Synthetic Aperture Radar: A Signal Processing Approach: A Signal Processing Approach*. Springer, 2012.
[68] J. Vanus, "The use of the adaptive noise cancellation for voice communication with the control system," *Int. J. Comput. Sci. Appl.*, vol. 8, no. 1, pp. 54–70, 2011.
[69] J. Vanus, M. Smolon, J. Koziorek, and R. Martinek, "Voice control of technical functions in smart home with KNX technology," in *Proc. 6th FTRA Int. Conf. Comput. Sci. Appl. (CSA)*, vol. 330, H. Y. Jeong, I. Stojmenovic, J. J. Park and G. Yi, Eds. Berlin, Germany: Springer-Verlag, 2015, pp. 455–462.
[70] J. Vanus and V. Styskala, "Application of optimal settings of the LMS adaptive filter for speech signal processing," in *Proc. Int. Multiconference Comput. Sci. Inf. Technol.*, Oct. 2010, pp. 767–774.
[71] J. Vanus, "Implementation of the adaptive filter for voice communications with control systems," in *Proc. TSO*, Prešov, Slovakia, 2009, pp. 144–147.
[72] D. Kuhlman, *A Python Book: Beginning Python, Advanced Python, and Python Exercises*. Lutz, FL, USA: Dave Kuhlman, 2009.
[73] L. Tulchak and A. Marchuk, "History of Python," Ph.D. dissertation, BHTY, Bathinda, Punjab, 2016.
[74] X. Shi, "Python for internet GIS applications," *Comput. Sci. Eng.*, vol. 9, no. 3, p. 56, 2007.
[75] G. Lindstrom, "Programming with Python," *IT Prof.*, vol. 5, no. 5, pp. 10–16, 2005.
[76] K. J. Millman and M. Aivazis, "Python for scientists and engineers," *Comput. Sci. Eng.*, vol. 13, no. 2, pp. 9–12, Mar./Apr. 2011.
[77] M. Hines, A. P. Davison, and E. Müller, "NEURON and Python," *Frontiers Neuroinform.*, vol. 3, p. 1, Jan. 2009.
[78] M. Abadi *et al.*, "TensorFlow: Large-scale machine learning on heterogeneous systems," Tech. Rep., 2015.
[79] C. Francois *et al.*, "Keras," Tech. Rep., 2015.
[80] P. Vidnerova, "RBF-keras: An RBF layer for keras library," Tech. Rep., 2019.

JAN VANUS was born in Czech Republic, in 1972. He received the degree in electrical engineering–measurement and control technology and the Ph.D. degree in technical cybernetics from the VSB—Technical University of Ostrava, Czech Republic, in 1996 and 2010, respectively. He defended his Ph.D. dissertation (Topic–Voice Communication with the Control System) at the VSB—Technical University of Ostrava. He currently works as an Assistant Professor with the Department of Cybernetics and Biomedical Engineering, FEI, VŠB—TU Ostrava. His research interests include smart home and smart home care within the IoT, speech signal processing, adaptive filters, neural networks, and wavelet transform.

OJAN MAJIDZADEH GORJANI was born in Tehran, Iran, in 1990. He received the B.S. degree in electrical engineering from the University of Nicosia, Nicosia, Cyprus, in 2016, and the M.S. degree in electrical engineering from the Wroclaw University of Science and Technology, Wroclaw, Poland, in 2018. He is currently pursuing the Ph.D. degree in cybernetics with the VSB—Technical University of Ostrava, Ostrava, Czech Republic. His research interests include artificial intelligence, big data analysis, and smart homes automation.

PETR DVORACEK was born in Bohumín, Czech Republic, in 1997. He received the bachelor's degree in electrical engineering from the VSB—Technical University of Ostrava, in 2019, where he is currently pursuing the master's degree. In 2017, he joined the Department of Nanotechnology, IT4I, VSB—Technical University of Ostrava, as a Junior Researcher. In 2018, he joined the Department of Cybernetics and Biomedical Engineering, as a Junior Programmer and a Researcher. His current research interests include machine learning algorithms for time series and image processing.

PETR BILIK was born in 1968. He received the master's degree in power electronics and the Ph.D. degree in technical cybernetics from the VSB—Technical University of Ostrava, in 1991 and 2004, respectively. From 2000 to 2012, he worked as the Head of the Power Quality Measurement System Department in commercial company. He is currently the Vice-Head of the Department of Cybernetics and Biomedical Engineering. His main research interests include automated test and measurement systems design, data acquisition, and signal processing.

JIRI KOZIOREK was born in Czech Republic, in 1973. He received the master's degree in measurement and control systems from the Faculty of Electrical Engineering and Computer Science, VSB—Technical University of Ostrava, in 1996. Since 1998, he has been working as an Assistant Professor with the VSB—TU Ostrava. During his Ph.D. studies, he was working in the area of distributed control system design. He defended his Ph.D. thesis, in 2005 (branch of study technical cybernetics). He became an Associate Professor in technical cybernetics, in 2008. Since 2009, he has been the Head of the Department of Cybernetics and Biomedical Engineering, VSB—TU Ostrava. He is the co-ordinator of several national and international research projects, typically in cooperation with industrial partners. His research interests include control system design, industrial communication, digitalization of industry, sensors, and non-electrical measurement.